nature portfolio

https://doi.org/10.1038/s41550-021-01381-5

Supplementary information

Transit detection of the long-period volatile-rich super-Earth ν^2 Lupi d with CHEOPS

In the format provided by the authors and unedited

Transit detection of the long-period volatile-rich super-Earth ν^2 Lupi d with *CHEOPS*

Visit	**Start date and time (UTC)**	**Duration (h)**	**Data points**	**Efficiency (%)**	**Planet(s)**
1	2020-04-04T15:13:16.9	11.56	526	55.9	b
2	2020-04-14T16:21:58.1	10.96	538	60.3	c
3	2020-04-16T03:59:45.7	11.60	545	57.7	b
4	2020-04-27T18:01:43.2	12.83	611	58.5	b
5	2020-06-08T21:33:50.9	11.65	504	53.1	c,d
6	2020-07-06T10:40:06.7	11.56	466	49.5	b,c

Supplementary Table 1. Log of *CHEOPS* observations of ν^2 Lupi.

Elements	**Abundances (dex)**
[Fe/H]	-0.34 ± 0.04
[Mg/H]	-0.14 ± 0.05
[Al/H]	-0.13 ± 0.02
[Si/H]	-0.23 ± 0.03
[Ca/H]	-0.24 ± 0.05
[Ti/H]	-0.17 ± 0.04
[Cr/H]	-0.32 ± 0.05
[Ni/H]	-0.35 ± 0.02
[α/H]	-0.19 ± 0.02

Supplementary Table 2. Detailed stellar abundances of ν^2 Lupi.

Parameters	**Priors**	**Description**
Physical parameters		
P_b (d)	$\mathcal{U}$(11.53, 11.63)	Orbital period of planet b
$T_{0,b}$ ($\mathrm{BJD_{TDB}}$)	$\mathcal{U}$(2458944.28, 2458944.44)	Mid-transit time of planet b
$r_{1,b}$	$\mathcal{U}$(0, 1)	Parametrization for p and b for planet b
$r_{2,b}$	$\mathcal{U}$(0, 1)	Parametrization for p and b for planet b
K_b (m/s)	$\mathcal{U}$(0, 10)	RV semi-amplitude for planet b
$\sqrt{e_b}\sin\omega_b$	$\mathcal{U}$(-1, 1) or fixed to 0 for the circular model	Parametrization for e and ω for planet b
$\sqrt{e_b}\cos\omega_b$	$\mathcal{U}$(-1, 1) or fixed to 0 for the circular model	Parametrization for e and ω for planet b
P_c (d)	$\mathcal{U}$(27.54, 27.64)	Orbital period of planet c
$T_{0,c}$ ($\mathrm{BJD_{TDB}}$)	$\mathcal{U}$(2458954.35, 2458954.47)	Mid-transit time of planet c
$r_{1,c}$	$\mathcal{U}$(0, 1)	Parametrization for p and b for planet c
$r_{2,c}$	$\mathcal{U}$(0, 1)	Parametrization for p and b for planet c
K_c (m/s)	$\mathcal{U}$(0, 10)	RV semi-amplitude for planet c
$\sqrt{e_c}\sin\omega_c$	$\mathcal{U}$(-1, 1) or fixed to 0 for the circular model	Parametrization for e and ω for planet c
$\sqrt{e_c}\cos\omega_c$	$\mathcal{U}$(-1, 1) or fixed to 0 for the circular model	Parametrization for e and ω for planet c
P_d (d)	$\mathcal{U}$(105, 110)	Orbital period of planet d
$T_{0,d}$ ($\mathrm{BJD_{TDB}}$)	$\mathcal{U}$(2459009.6, 2459010.0)	Mid-transit time of planet d
$r_{1,d}$	$\mathcal{U}$(0, 1)	Parametrization for p and b for planet d
$r_{2,d}$	$\mathcal{U}$(0, 1)	Parametrization for p and b for planet d
K_d (m/s)	$\mathcal{U}$(0, 10)	RV semi-amplitude for planet d
$\sqrt{e_d}\sin\omega_d$	$\mathcal{U}$(-1, 1) or fixed to 0 for the circular model	Parametrization for e and ω for planet d
$\sqrt{e_d}\cos\omega_d$	$\mathcal{U}$(-1, 1) or fixed to 0 for the circular model	Parametrization for e and ω for planet d
$\rho_\star$ (kg/m^3)	$\mathcal{N}$(1035, 76^2)	Stellar density
$q_{1,TESS}$	$\mathcal{U}$(0, 1)	Quadratic limb-darkening parametrization for *TESS*
$q_{2,TESS}$	$\mathcal{U}$(0, 1)	Quadratic limb-darkening parametrization for *TESS*
$q_{1,CHEOPS}$	$\mathcal{U}$(0, 1)	Quadratic limb-darkening parametrization for *CHEOPS*
$q_{2,CHEOPS}$	$\mathcal{U}$(0, 1)	Quadratic limb-darkening parametrization for *CHEOPS*
Nuisance parameters		
σ_{TESS} (ppm)	$\mathcal{J}$(1, 1000); $\mathcal{N}$(122.7, 1.1^2)	Extra jitter term for *TESS*
M_{TESS}	$\mathcal{N}$(0, 0.1^2); $\mathcal{N}$(-0.000004, 0.000003^2)	Relative flux offset for *TESS*
$\sigma_{GP,TESS}$ (ppm)	$\mathcal{J}$(0.1, 10^4); $\mathcal{N}$(31, 2^2)	Amplitude of the Matérn GP for *TESS*
$\rho_{GP,TESS}$	$\mathcal{J}$(10^{-4}, 10^4); $\mathcal{N}$(0.055, 0.010^2)	Length-scale of the Matérn GP for *TESS*
$\sigma_{CHEOPS1}$ (ppm)	$\mathcal{J}$(1, 1000); $\mathcal{N}$(26.3, 1.9^2)	Extra jitter term for the 1$^{\rm st}$ *CHEOPS* visit
$M_{CHEOPS1}$	$\mathcal{N}$(0, 0.1^2); $\mathcal{N}$(-0.000027, 0.000061^2)	Relative flux offset for the 1$^{\rm st}$ *CHEOPS* visit
$\theta_{0,CHEOPS1}$	$\mathcal{U}$(-1, 1); $\mathcal{N}$(-0.000040, 0.000088^2)	sin(ϕ) regression coefficient for the 1$^{\rm st}$ *CHEOPS* visit
$\theta_{1,CHEOPS1}$	$\mathcal{U}$(-1, 1); $\mathcal{N}$(-0.000092, 0.000062^2)	cos(ϕ) regression coefficient for the 1$^{\rm st}$ *CHEOPS* visit
$\theta_{2,CHEOPS1}$	$\mathcal{U}$(-1, 1); $\mathcal{N}$(0.000059, 0.000064^2)	sin(2ϕ) regression coefficient for the 1$^{\rm st}$ *CHEOPS* visit
$\theta_{3,CHEOPS1}$	$\mathcal{U}$(-1, 1); $\mathcal{N}$(-0.000081, 0.000031^2)	cos(2ϕ) regression coefficient for the 1$^{\rm st}$ *CHEOPS* visit
$\theta_{4,CHEOPS1}$	$\mathcal{U}$(-1, 1); $\mathcal{N}$(0.000048, 0.000018^2)	sin(3ϕ) regression coefficient for the 1$^{\rm st}$ *CHEOPS* visit
$\theta_{5,CHEOPS1}$	$\mathcal{U}$(-1, 1); $\mathcal{N}$(-0.000019, 0.000030^2)	cos(3ϕ) regression coefficient for the 1$^{\rm st}$ *CHEOPS* visit
$\sigma_{CHEOPS2}$ (ppm)	$\mathcal{J}$(1, 1000); $\mathcal{N}$(26.5, 2.0^2)	Extra jitter term for the 2$^{\rm nd}$ *CHEOPS* visit
$M_{CHEOPS2}$	$\mathcal{N}$(0, 0.1^2); $\mathcal{N}$(0.000115, 0.000045^2)	Relative flux offset for the 2$^{\rm nd}$ *CHEOPS* visit
$\theta_{0,CHEOPS2}$	$\mathcal{U}$(-1, 1); $\mathcal{N}$(0.000149, 0.000055^2)	sin(ϕ) regression coefficient for the 2$^{\rm nd}$ *CHEOPS* visit
$\theta_{1,CHEOPS2}$	$\mathcal{U}$(-1, 1); $\mathcal{N}$(-0.000199, 0.000059^2)	cos(ϕ) regression coefficient for the 2$^{\rm nd}$ *CHEOPS* visit
$\theta_{2,CHEOPS2}$	$\mathcal{U}$(-1, 1); $\mathcal{N}$(0.000189, 0.000053^2)	sin(2ϕ) regression coefficient for the 2$^{\rm nd}$ *CHEOPS* visit
$\theta_{3,CHEOPS2}$	$\mathcal{U}$(-1, 1); $\mathcal{N}$(-0.000013, 0.000017^2)	cos(2ϕ) regression coefficient for the 2$^{\rm nd}$ *CHEOPS* visit
$\theta_{4,CHEOPS2}$	$\mathcal{U}$(-1, 1); $\mathcal{N}$(0.000044, 0.000021^2)	sin(3ϕ) regression coefficient for the 2$^{\rm nd}$ *CHEOPS* visit
$\theta_{5,CHEOPS2}$	$\mathcal{U}$(-1, 1); $\mathcal{N}$(0.000043, 0.000021^2)	cos(3ϕ) regression coefficient for the 2$^{\rm nd}$ *CHEOPS* visit
$\sigma_{CHEOPS3}$ (ppm)	$\mathcal{J}$(1, 1000); $\mathcal{N}$(26.5, 1.9^2)	Extra jitter term for the 3$^{\rm rd}$ *CHEOPS* visit
$M_{CHEOPS3}$	$\mathcal{N}$(0, 0.1^2); $\mathcal{N}$(-0.000029, 0.000008^2)	Relative flux offset for the 3$^{\rm rd}$ *CHEOPS* visit
$\theta_{0,CHEOPS3}$	$\mathcal{U}$(-1, 1); $\mathcal{N}$(-0.000039, 0.000011^2)	sin(ϕ) regression coefficient for the 3$^{\rm rd}$ *CHEOPS* visit
$\theta_{1,CHEOPS3}$	$\mathcal{U}$(-1, 1); $\mathcal{N}$(-0.000003, 0.000011^2)	cos(ϕ) regression coefficient for the 3$^{\rm rd}$ *CHEOPS* visit
$\sigma_{CHEOPS4}$ (ppm)	$\mathcal{J}$(1, 1000); $\mathcal{N}$(38.1, 3.4^2)	Extra jitter term for the 4$^{\rm th}$ *CHEOPS* visit
$M_{CHEOPS4}$	$\mathcal{N}$(0, 0.1^2); $\mathcal{N}$(-0.000099, 0.000014^2)	Relative flux offset for the 4$^{\rm th}$ *CHEOPS* visit
$\theta_{0,CHEOPS4}$	$\mathcal{U}$(-1, 1); $\mathcal{N}$(-0.000048, 0.000012^2)	sin(ϕ) regression coefficient for the 4$^{\rm th}$ *CHEOPS* visit

$\theta_{1,CHEOPS4}$	$\mathcal{U}$(-1, 1); $\mathcal{N}$(0.000084, 0.000022^2)	cos(ϕ) regression coefficient for the 4$^{\rm th}$ *CHEOPS* visit
$\theta_{2,CHEOPS4}$	$\mathcal{U}$(-1, 1); $\mathcal{N}$(0.000003, 0.000014^2)	sin(2ϕ) regression coefficient for the 4$^{\rm th}$ *CHEOPS* visit
$\theta_{3,CHEOPS4}$	$\mathcal{U}$(-1, 1); $\mathcal{N}$(0.000024, 0.000013^2)	cos(2ϕ) regression coefficient for the 4$^{\rm th}$ *CHEOPS* visit
$\sigma_{CHEOPS5}$ (ppm)	$\mathcal{J}$(1, 1000); $\mathcal{N}$(33.3, 3.9^2)	Extra jitter term for the 5$^{\rm th}$ *CHEOPS* visit
$M_{CHEOPS5}$	$\mathcal{N}$(0, 0.1^2); $\mathcal{N}$(-0.000004, 0.000013^2)	Relative flux offset for the 5$^{\rm th}$ *CHEOPS* visit
$\theta_{0,CHEOPS5}$	$\mathcal{U}$(-1, 1); $\mathcal{N}$(0.000003, 0.000011^2)	sin(ϕ) regression coefficient for the 5$^{\rm th}$ *CHEOPS* visit
$\theta_{1,CHEOPS5}$	$\mathcal{U}$(-1, 1); $\mathcal{N}$(0.000037, 0.000014^2)	cos(ϕ) regression coefficient for the 5$^{\rm th}$ *CHEOPS* visit
$\sigma_{CHEOPS6}$ (ppm)	$\mathcal{J}$(1, 1000); $\mathcal{N}$(34.8, 3.9^2)	Extra jitter term for the 6$^{\rm th}$ *CHEOPS* visit
$M_{CHEOPS6}$	$\mathcal{N}$(0, 0.1^2); $\mathcal{N}$(-0.000062, 0.000011^2)	Relative flux offset for the 6$^{\rm th}$ *CHEOPS* visit
$\theta_{0,CHEOPS6}$	$\mathcal{U}$(-1, 1); $\mathcal{N}$(0.000021, 0.000017^2)	sin(ϕ) regression coefficient for the 6$^{\rm th}$ *CHEOPS* visit
$\theta_{1,CHEOPS6}$	$\mathcal{U}$(-1, 1); $\mathcal{N}$(0.000064, 0.000011^2)	cos(ϕ) regression coefficient for the 6$^{\rm th}$ *CHEOPS* visit
$S0_{GP,CHEOPS}$	$\mathcal{J}$(10^{-20}, 10^{20}); $\mathcal{N}$(5.2 10^{-12},(6.0 10^{-13})^2)	Characteristic power of the SHO GP for *CHEOPS*
$\omega0_{GP,CHEOPS}$	$\mathcal{J}$(10^{-5}, 10^5); $\mathcal{N}$(838, 60^2)	Characteristic frequency of the SHO GP for *CHEOPS*
$\sigma_{\rm HARPS-pre}$ (m/s)	$\mathcal{J}$(0.01, 10); $\mathcal{N}$(1.34, 0.07^2)	Extra jitter term for HARPS pre-upgrade
$\mu_{\rm HARPS-pre}$ (m/s)	$\mathcal{U}$(-68720, -68700); $\mathcal{N}$(-68709.02, 0.09^2)	Systemic velocity for HARPS pre-upgrade
$\sigma_{\rm HARPS-post}$ (m/s)	$\mathcal{J}$(0.01, 10); $\mathcal{N}$(0.20, 0.58^2)	Extra jitter term for HARPS post-upgrade
$\mu_{\rm HARPS-post}$ (m/s)	$\mathcal{U}$(-68705, -68685); $\mathcal{N}$(-68695.10, 0.36^2)	Systemic velocity for HARPS post-upgrade

Supplementary Table 3. Priors used in our data analyses with `juliet`. $\mathcal{N}(\mu, \sigma^2)$ represents a normal distribution of mean μ and variance σ^2. $\mathcal{U}(a, b)$ represents a uniform distribution between a and b. $\mathcal{J}(a, b)$ represents a Jeffrey's prior (i.e. a log-uniform distribution) between a and b. For the nuisance parameters, two prior distributions are given. The first ones are the wide priors that we assumed for the preliminary individual analyses of each dataset. The second ones are the normal priors that we assumed in our global analysis (to aid convergence), based on the results from the preliminary individual analyses.

Models	**Δ ln** Z
Reference model:	
3 planets, circular orbits for all planets, *CHEOPS* single transit caused by d	$-$
Tests for eccentricities:	
Eccentric orbit for b, circular orbits for c and d	-0.9
Eccentric orbit for c, circular orbits for b and d	-1.7
Eccentric orbit for d, circular orbits for b and c	-0.9
Eccentric orbits for all planets	-3.6
Tests for a fourth planet and origin of the CHEOPS single transit:	
4 planets (P_e=485d), *CHEOPS* single transit caused by e, d not transiting	-2.5
4 planets (P_e=485d), *CHEOPS* single transit caused by d, e not transiting	$+0.6$

Supplementary Table 4. Comparison of different models based on their Bayesian log evidence. Based on these tests, we adopted the reference model as our nominal solution (3 planets with circular orbits, single *CHEOPS* transit caused by planet d).

Parameters	Ref. [1] (*TESS*+RVs)	***TESS*** (+RVs)	***CHEOPS*** (+RVs)	**Global analysis** (*TESS*+*CHEOPS*+RVs)
Planet b				
$R_p/R_\star$	$0.01343^{+0.00044}_{-0.00045}$	$0.01323^{+0.00075}_{-0.00074}$	$0.01439^{+0.00040}_{-0.00041}$	$0.01428^{+0.00036}_{-0.00038}$
R_p ($R_\oplus$)	$1.482^{+0.058}_{-0.056}$	1.527 ± 0.090	1.661 ± 0.055	$1.648^{+0.052}_{-0.051}$
b ($R_\star$)	$0.41^{+0.12}_{-0.20}$	$0.38^{+0.15}_{-0.22}$	$0.48^{+0.09}_{-0.16}$	$0.47^{+0.09}_{-0.16}$
W (hours)	$3.936^{+0.115}_{-0.108}$	$4.25^{+0.25}_{-0.34}$	$3.95^{+0.14}_{-0.08}$	$3.940^{+0.103}_{-0.064}$
T_0 ($\mathrm{BJD_{TDB}} - 2,450,000$)	$8631.7672^{+0.0023}_{-0.0022}$	$8631.7723^{+0.0036}_{-0.0050}$	$8944.3718^{+0.0016}_{-0.0026}$	$8944.3724^{+0.0015}_{-0.0019}$
P (days)	$11.57779^{+0.00091}_{-0.0011}$	$11.57748^{+0.00103}_{-0.00124}$	$11.57822^{+0.00045}_{-0.00061}$	$11.57795^{+0.00009}_{-0.00014}$
e	$0.079^{+0.068}_{-0.053}$	$0.098^{+0.076}_{-0.064}$	$0.066^{+0.058}_{-0.045}$	$0.076^{+0.047}_{-0.046}$
Planet c				
$R_p/R_\star$	0.02363 ± 0.00052	$0.0249^{+0.0012}_{-0.0010}$	$0.02551^{+0.00055}_{-0.00051}$	$0.02527^{+0.00046}_{-0.00050}$
R_p ($R_\oplus$)	$2.608^{+0.078}_{-0.077}$	$2.87^{+0.14}_{-0.13}$	$2.944^{+0.084}_{-0.079}$	$2.918^{+0.074}_{-0.077}$
b ($R_\star$)	$0.854^{+0.013}_{-0.016}$	$0.874^{+0.012}_{-0.013}$	0.876 ± 0.010	0.873 ± 0.010
W (hours)	$3.209^{+0.058}_{-0.053}$	3.24 ± 0.11	$3.242^{+0.041}_{-0.038}$	$3.254^{+0.039}_{-0.033}$
T_0 ($\mathrm{BJD_{TDB}} - 2,450,000$)	$8650.8947^{+0.0011}_{-0.0010}$	$8650.8959^{+0.0013}_{-0.0012}$	$8954.40959^{+0.00067}_{-0.00070}$	$8954.40987^{+0.00051}_{-0.00054}$
P (days)	$27.5909^{+0.0028}_{-0.0031}$	$27.5911^{+0.0029}_{-0.0034}$	$27.59255^{+0.00045}_{-0.00048}$	27.59220 ± 0.00011
e	$0.037^{+0.039}_{-0.026}$	$0.038^{+0.042}_{-0.027}$	$0.022^{+0.027}_{-0.016}$	$0.022^{+0.026}_{-0.015}$

Supplementary Table 5. Comparison between the results of different data analyses for some key transit parameters of the planets ν^2 Lupi b and c. The second column presents the values reported by ref. [1] based on their analysis of the *TESS* and RV data. In the third column, we report the results of our own analysis of this same dataset. The fourth column gives the results of our analysis of the six *CHEOPS* visits together with the RVs, while the fifth column lists the results from our global analysis of all the data. We assumed eccentric orbits for these analyses, to allow a direct comparison with the results of ref. [1]. However, we note that circular orbits are actually favored for all the planets (see section "Global data analysis" and Table 1 for our nominal solution).

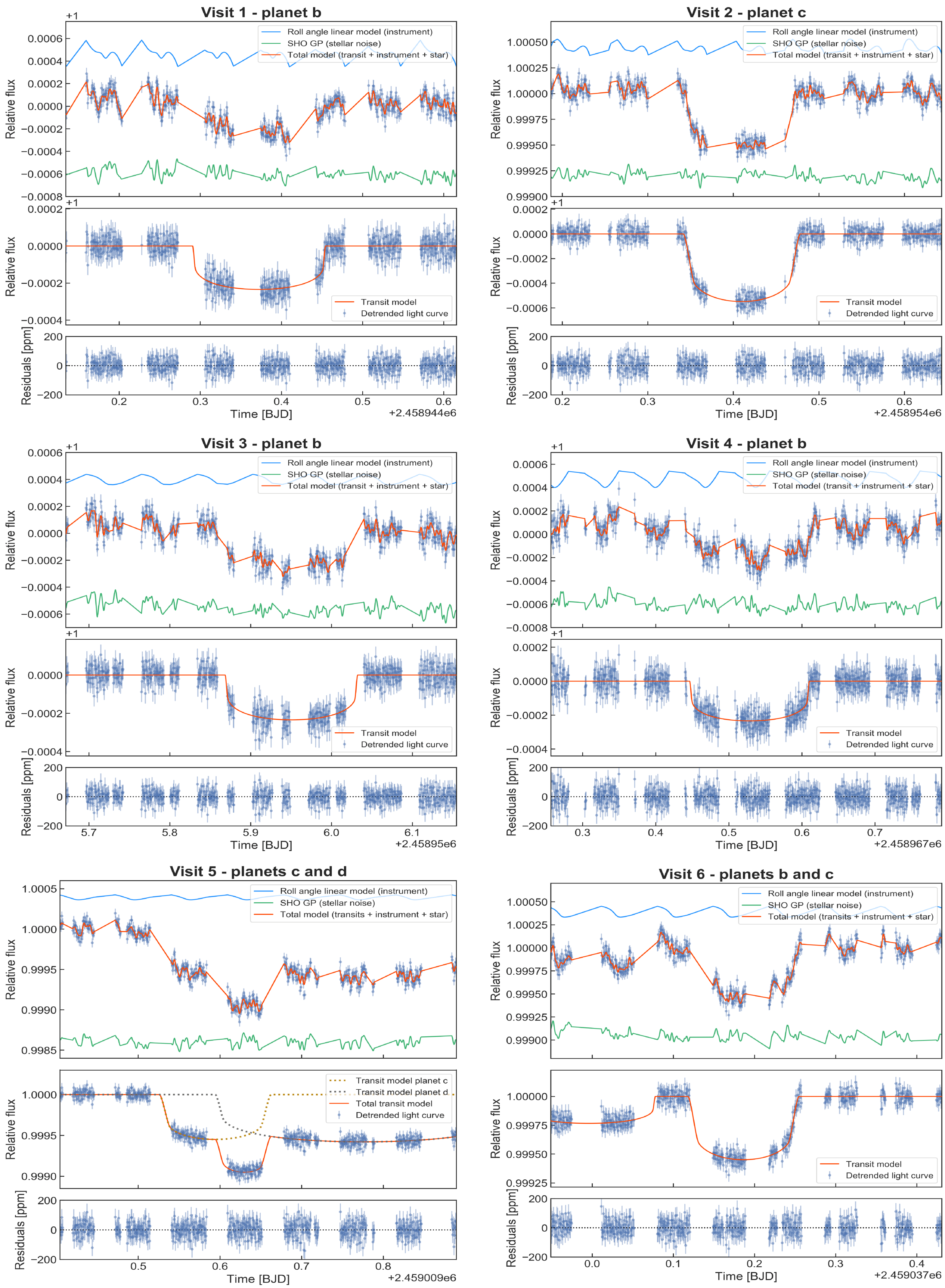

Supplementary Figure 1. Individual *CHEOPS* light curves. For each visit, the top panel shows the raw light curve (blue points with error bars), together with the best-fit instrumental noise (blue curve shifted vertically for visualisation), stellar noise (green curve shifted vertically), and total (transit + instrument + stellar noise, orange line) models. The second panel shows the light curve corrected from the best-fit instrumental and stellar noise models, together with the best-fit transit model. The bottom panel shows the residuals. The error bars correspond to the quadratic sum of the formal photometric errors and the fitted extra jitter term.

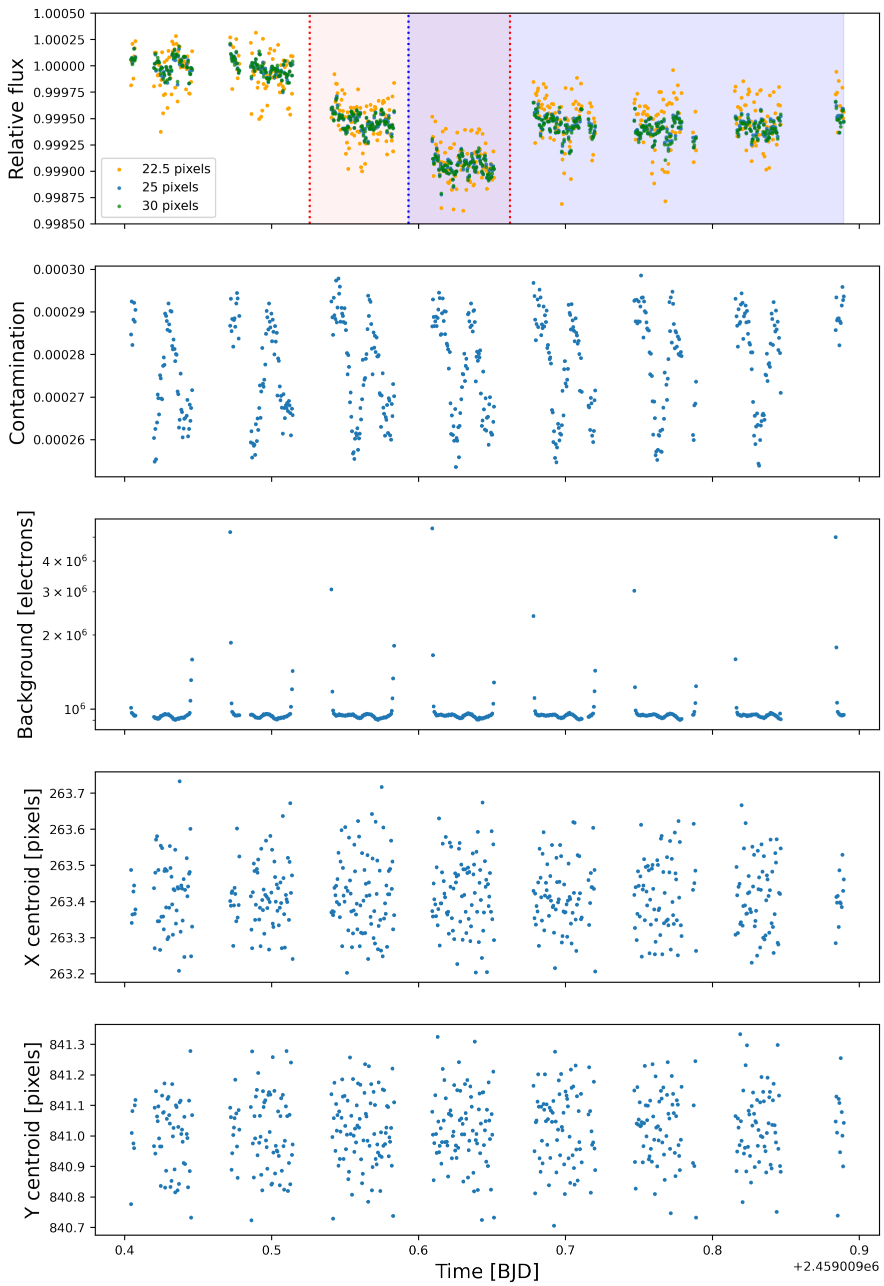

Supplementary Figure 2. Fifth *CHEOPS* visit. *Upper panel:* Raw light curves obtained for three different photometric apertures. All the light curves show an unexpected ∼500 ppm transit-like flux drop which started during the targeted transit of planet c (transit window indicated as a red shaded region) and lasted for the rest of the visit (blue shaded region). This signal does not show any correlation with instrumental or environmental parameters, of which the main ones are shown in the other panels. *Second panel:* Contamination from nearby stars entering the photometric aperture (25 pixels), relative to the target's flux. *Third panel:* Background (in electrons). Note that it is higher right before/after Earth occultations due to stray light. *Fourth and fifth panels:* x- and y- position of the target's PSF centroid on the CCD.

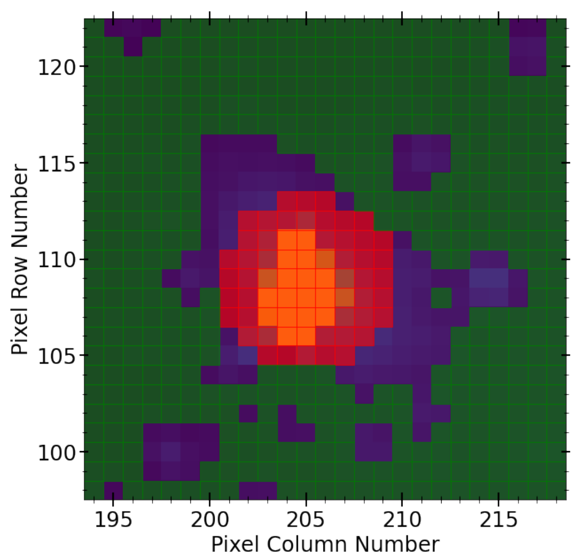

Supplementary Figure 3. Sample *TESS* target pixel file and masks used to measure the target flux (red) and background (green). For the background, we used pixels with median fluxes lower than one standard deviation above the overall median of the target pixel file.

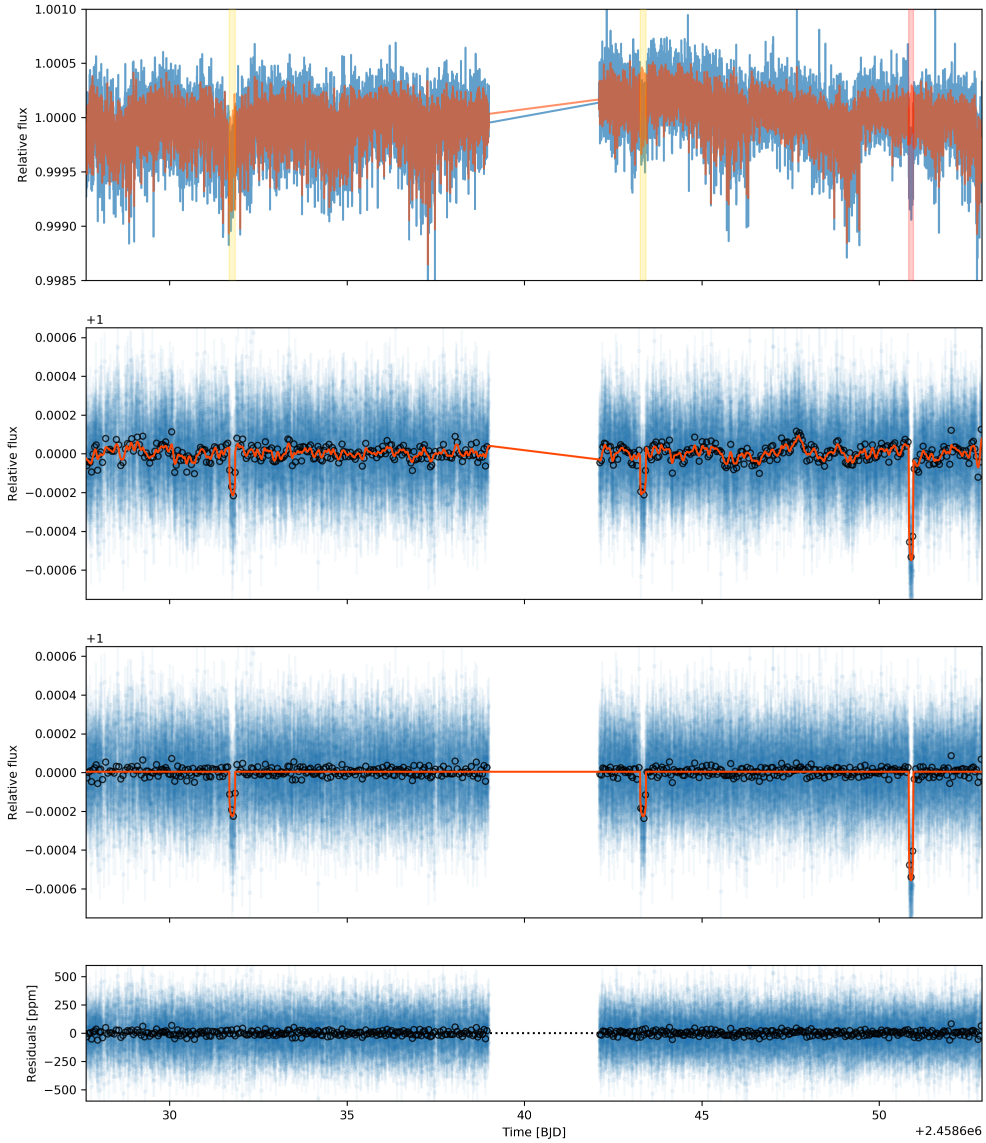

Supplementary Figure 4. *TESS* photometry of ν^2 Lupi. *Upper panel:* Raw photometry (in blue) along with our best-fit linear regression model (in orange). The locations of the two transits of planet b and single transit of planet c are indicated as yellow and red shaded regions, respectively. *Second panel:* Light curve (blue dots with error bars) corrected for most instrumental systematics that we used in our global analysis. The orange line shows our best-fit model which includes both the transits of planets b and c, and the GP model used to account for the remaining photometric variability. The black open circles show the light curve binned into 1-hour intervals. *Third panel:* Light curve obtained after subtracting the GP component of our model, together with our best-fit transit model. *Lower panel:* Corresponding residuals. For all panels, the error bars of the data points include the fitted extra jitter term added in quadrature.

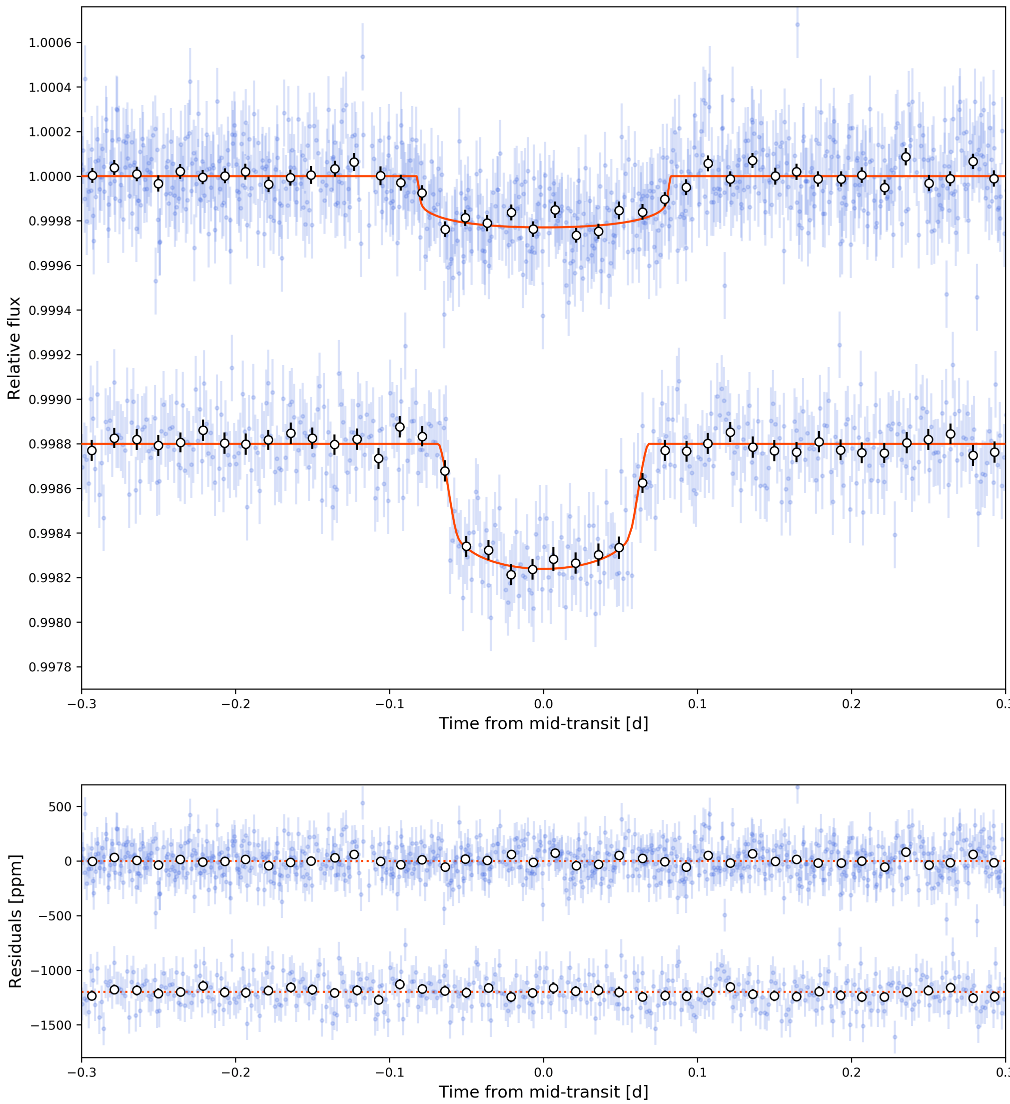

Supplementary Figure 5. *Upper panel:* Corrected and phase-folded *TESS* transit photometry of ν^2 Lupi b (top) and c (bottom). The blue dots show the unbinned measurements, with error bars corresponding to the quadratic sum of the formal photometric errors and the fitted extra jitter term. Open circles show the light curves binned into 20-minute intervals, with error bars corresponding to the standard deviation of the data for each bin. *Lower panel:* Corresponding residuals.

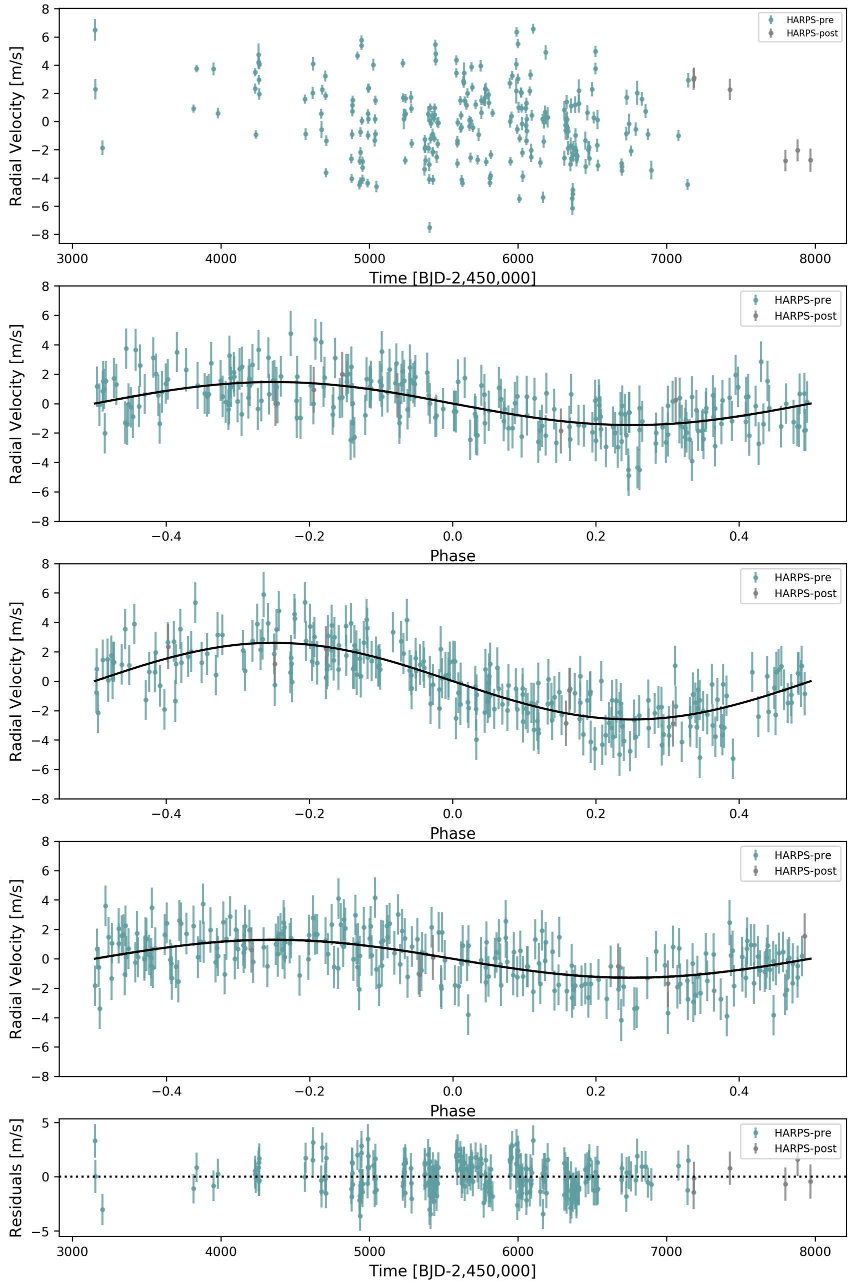

Supplementary Figure 6. HARPS radial velocities of ν^2 Lupi used in our analysis. Measurements obtained before the instrument upgrade are shown in blue, while those obtained after are shown in grey. *Upper panel:* The RVs are shown as a function of Barycentric Julian Date. The *second*, *third*, and *fourth panels* show the measurements folded on the orbital periods of planets b, c, and d, respectively, together with the respective best-fit RV models (solid lines). For each of these panels, the RVs were corrected for the signals of the other two planets, so that only the signal of the considered planet is visible. *Lower panel:* Residuals around the best-fit solution. For the upper panel, the error bars are the formal measurement uncertainties. For the other panels, the error bars are the quadratic sum of the measurement uncertainties and the fitted extra jitter term.

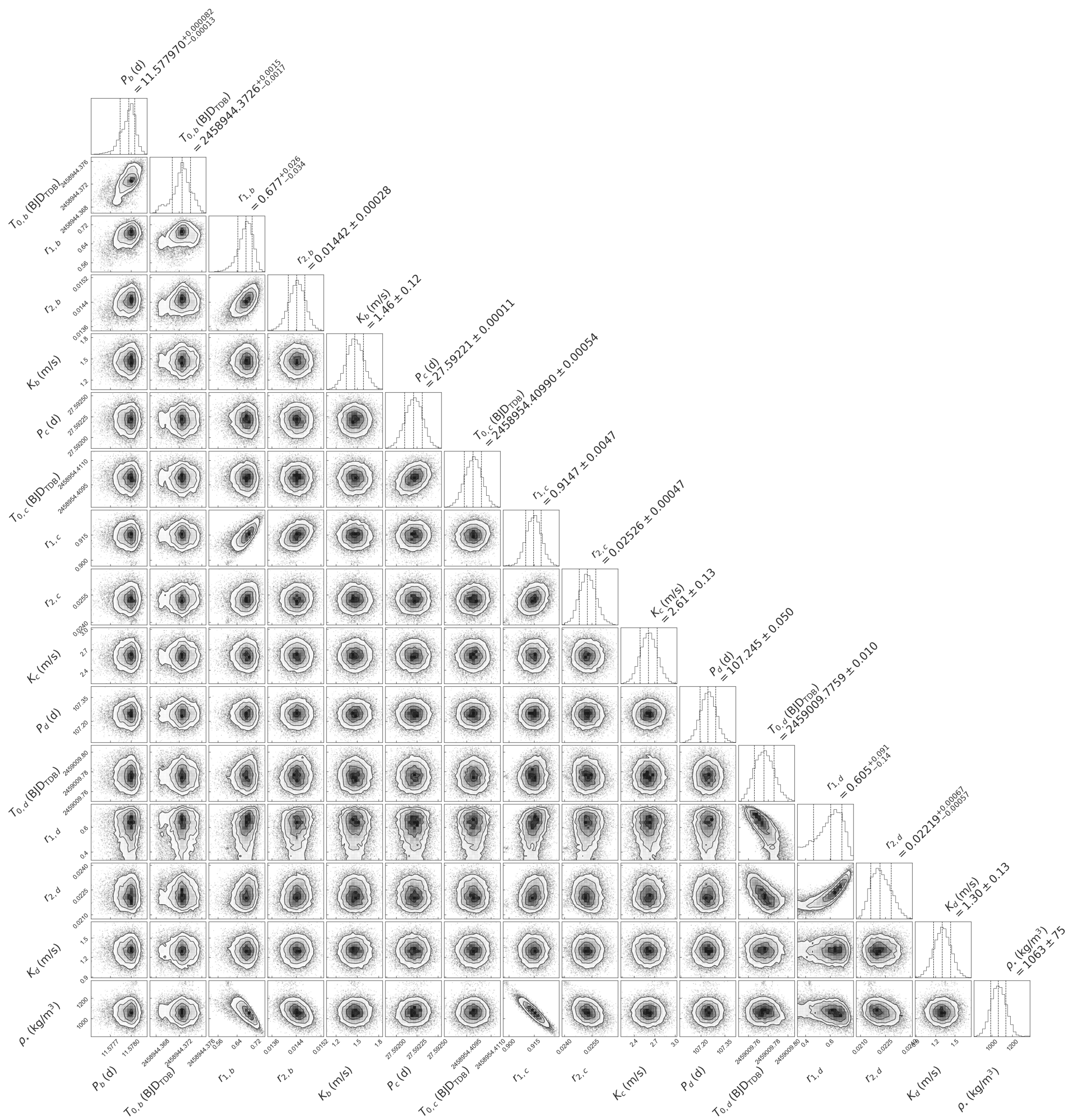

Supplementary Figure 7. Posterior distributions of the main fitted parameters of our global analysis. Shown are the orbital period P, the mid-transit time T_0, the parameters r_1 and r_2 (parametrization of the planet-to-star radius ratio $R_p/R_\star$ and the impact parameter b), and the RV semi-amplitude K of each planet, as well as the stellar density $\rho_\star$. This plot was made using the `corner`[2] python package.

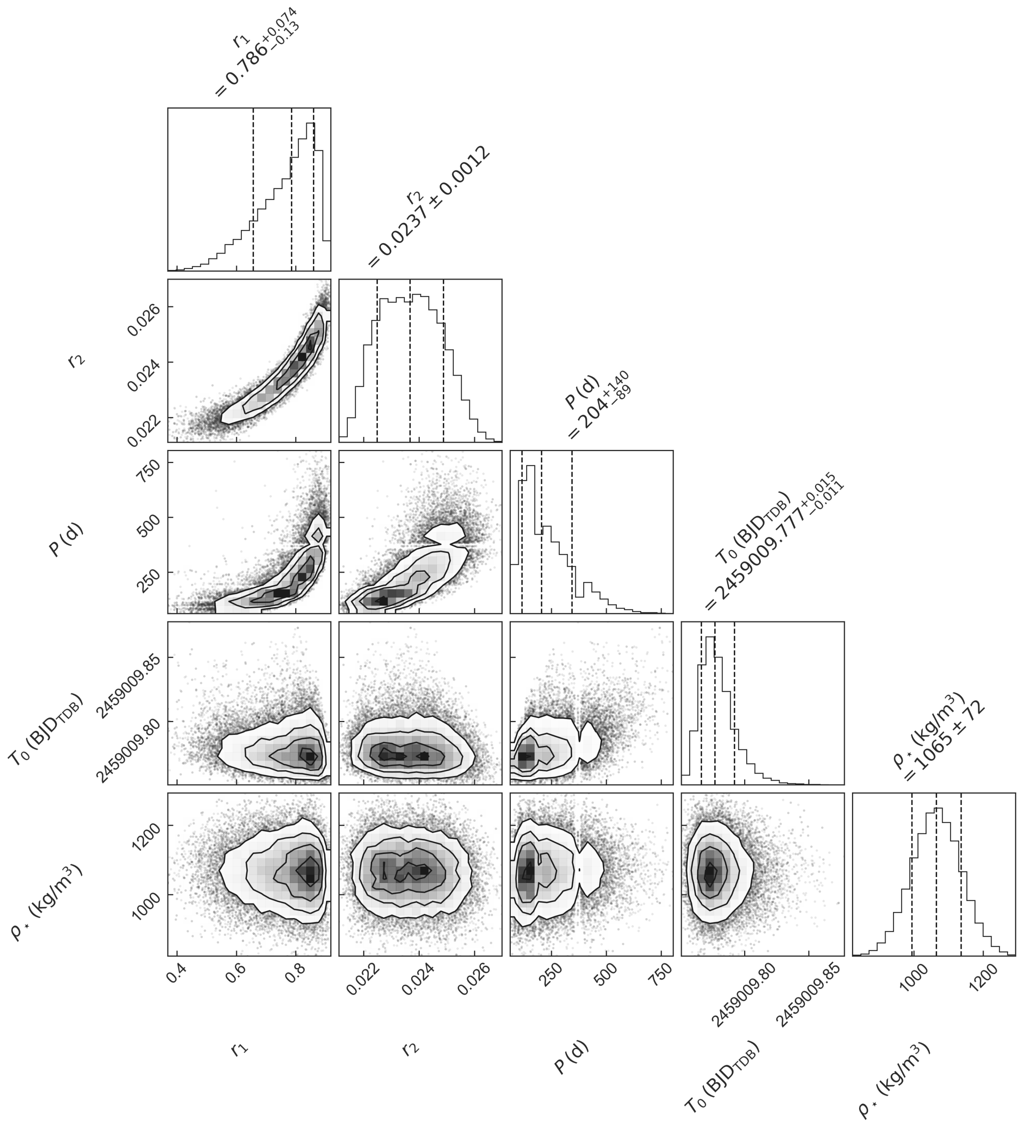

Supplementary Figure 8. Posterior distributions of the transit parameters corresponding to the planet that caused the *CHEOPS* single transit event, as constrained by a combined analysis of all the photometry (*CHEOPS* and *TESS*). The goal here is to assess the constraints brought by the photometry on the orbital period of the transiting object. Shown are the orbital period P, the mid-transit time T_0, the parameters r_1 and r_2 (parametrization of the planet-to-star radius ratio $R_p/R_\star$ and the impact parameter b), as well as the stellar density $\rho_\star$. This plot was made using the `corner`[2] python package.

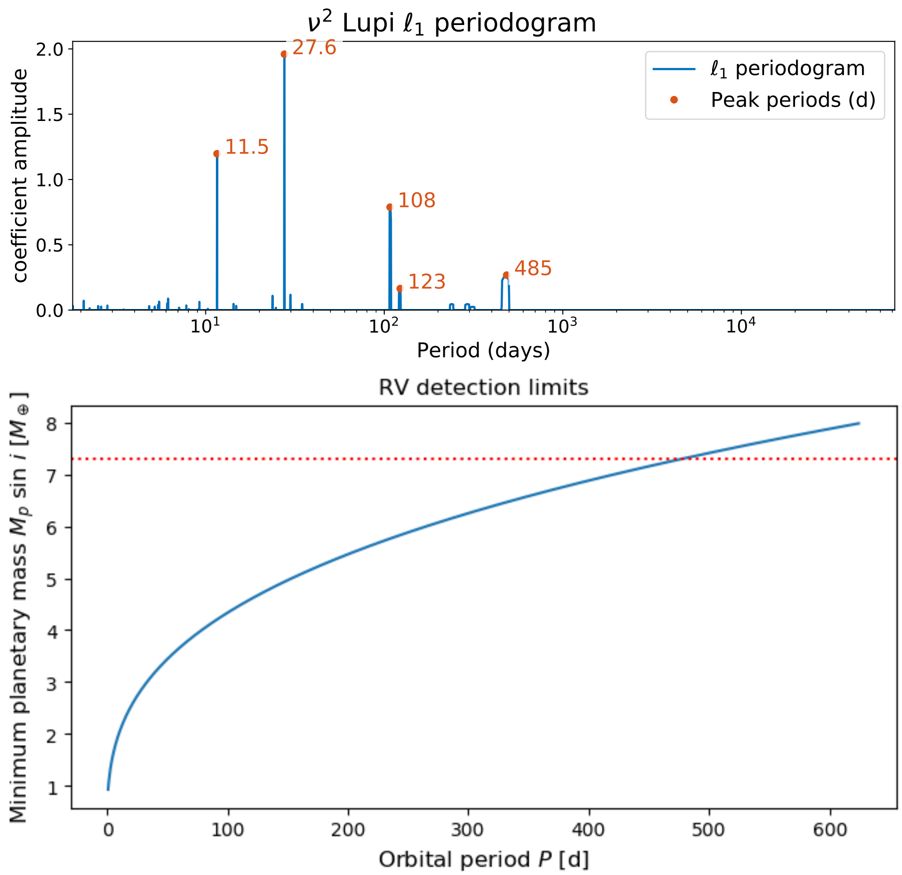

Supplementary Figure 9. *Top:* ℓ_1-periodogram of the HARPS radial velocities. *Bottom:* Approximate detection limits of the HARPS radial velocities. Any planet located above the blue curve should have been confidently detected. The red dotted line indicates the mass of $\sim$7.3 $M_\oplus$ estimated for the planet that transited during the fifth *CHEOPS* visit, based on its radius (as measured from the transit depth) and the empirical mass-radius relationship of ref. [3].

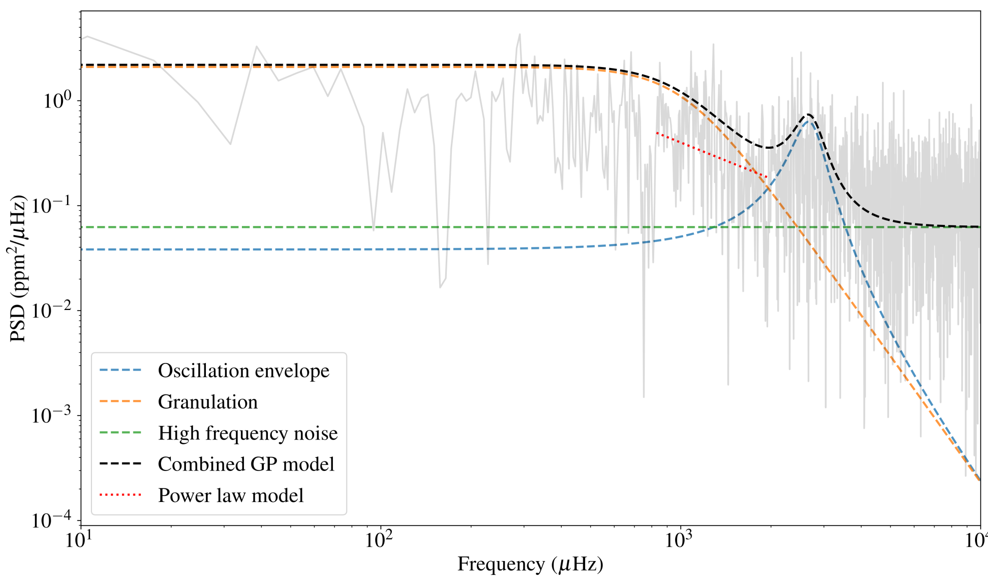

Supplementary Figure 10. Power spectral density (grey) of the photometric residuals obtained after subtracting the best-fit transit and instrumental models from the *CHEOPS* light curves. Dashed lines represent our best-fit models for the different components of the flicker noise, using the GP regression framework of ref. [4]. The red dotted line indicates the slope of the granulation noise when described with a power-law model.

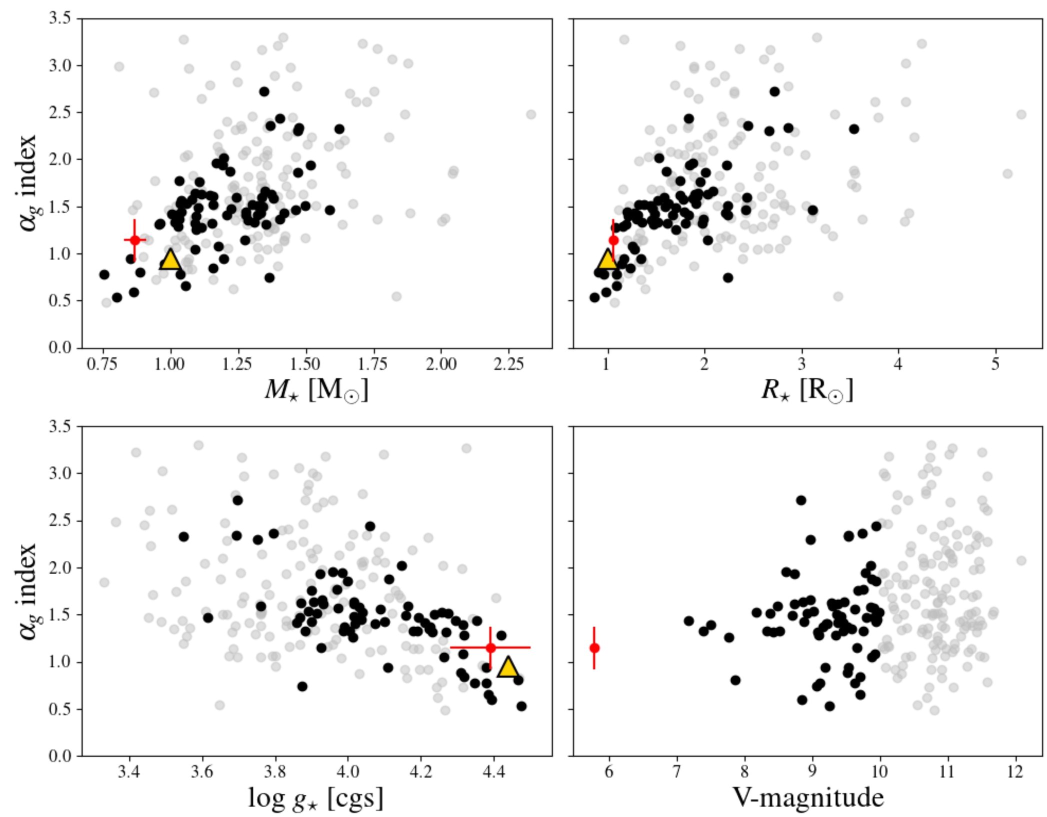

Supplementary Figure 11. *From left to right and top to bottom:* Estimated flicker index associated to granulation as a function of the stellar mass, radius, surface gravity, and apparent V-magnitude. Black (resp. grey) dots represent the indices inferred from *Kepler* data (see ref. [5]) for stars with magnitudes below (resp. above) 10. The yellow triangle represents the flicker index inferred for the Sun from *SOHO/VIRGO* solar data. The red dot with error bars indicates the value obtained for ν^2 Lupi with *CHEOPS*.

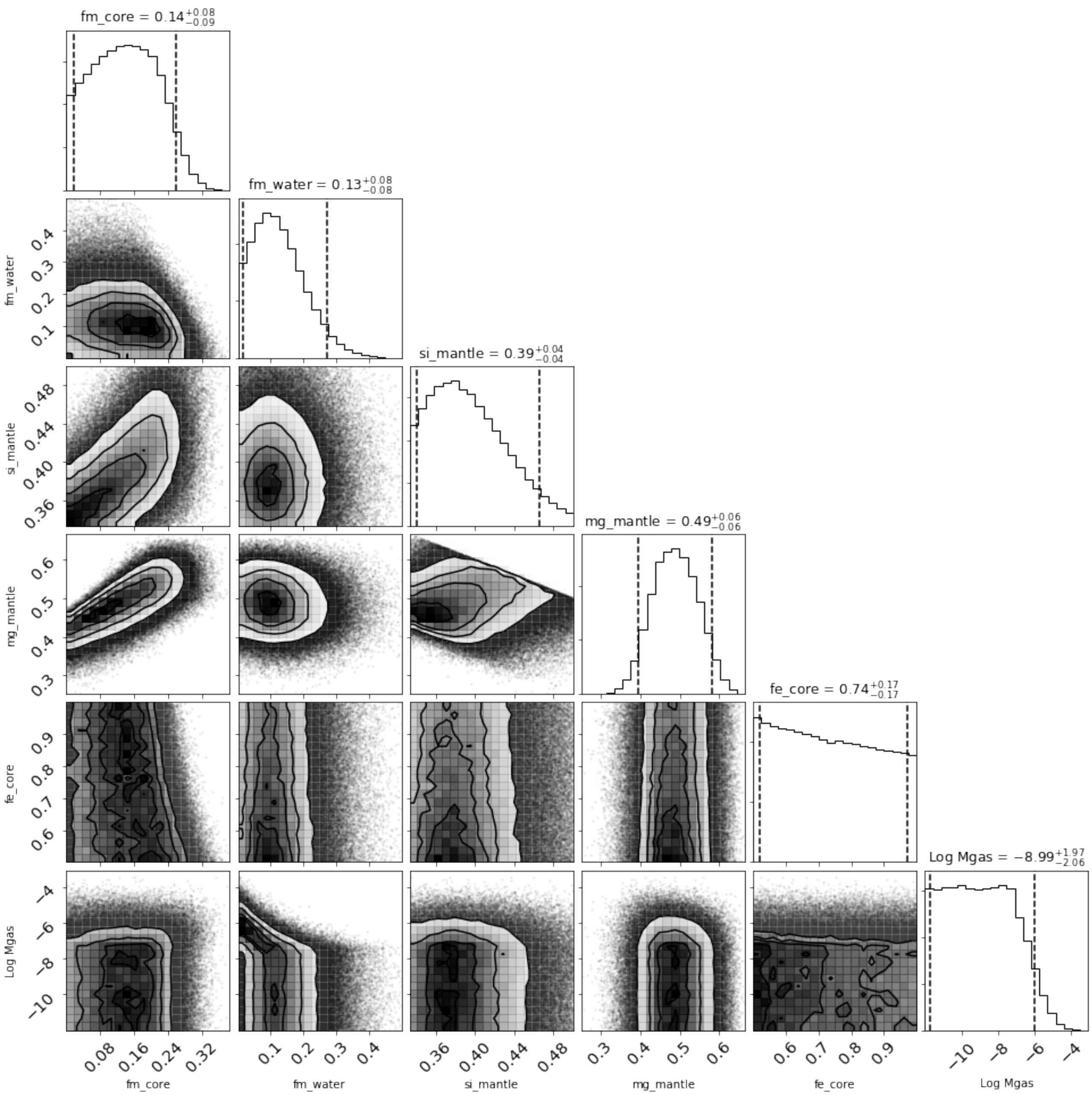

Supplementary Figure 12. Posterior distributions of the main internal structure parameters of planet b. Shown are the mass fractions of the core and water layer (relative to the total amount of heavy elements), the molar fractions of Si and Mg in the mantle, the molar fraction of iron in the core, and the mass of the gas layer. The numbers at the top of each column refer to the mean values and the 5% and 95% percentiles.

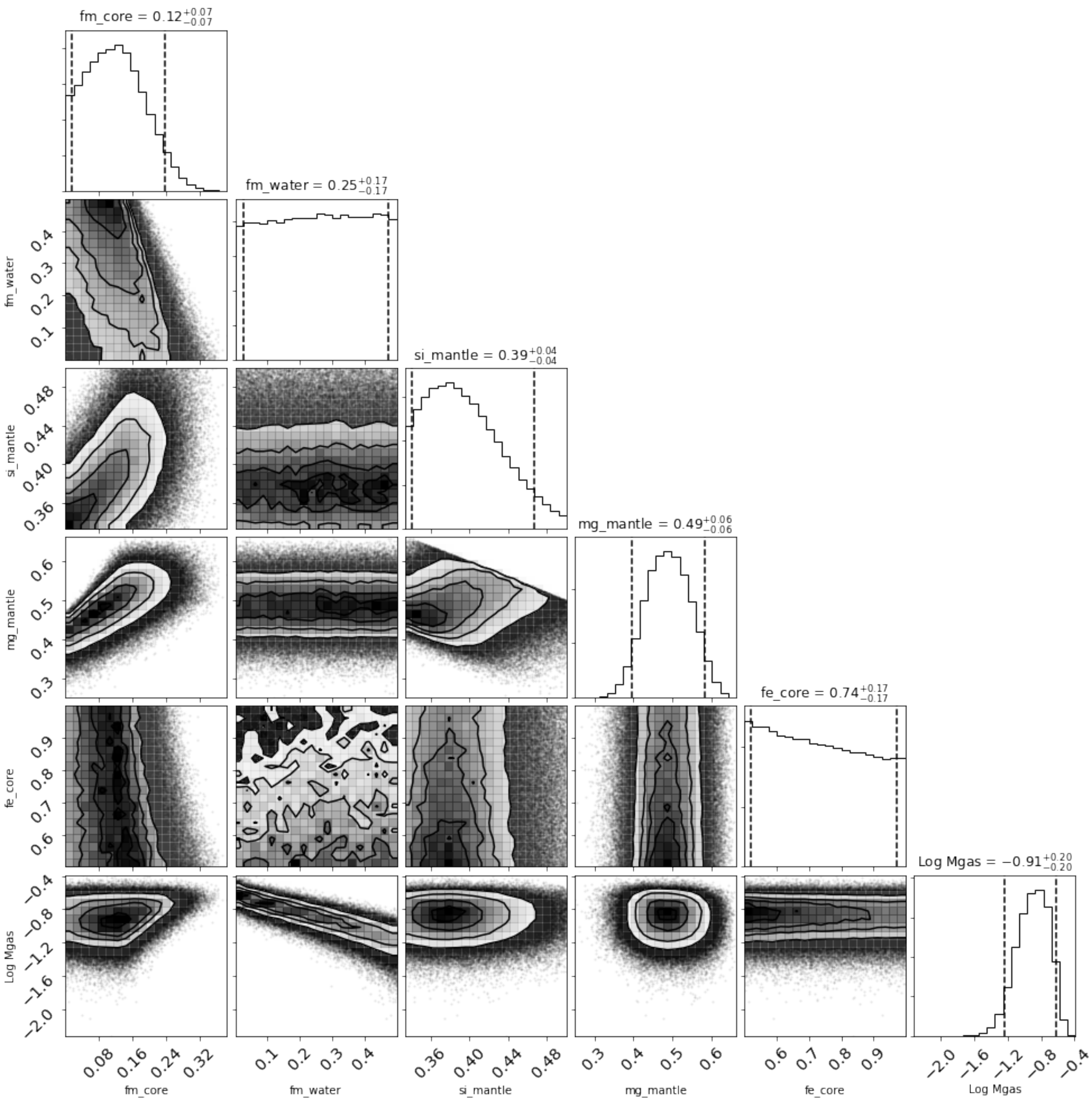

Supplementary Figure 13. Posterior distributions of the main internal structure parameters of planet c. The parameters are the same as in Supplementary Figure 12.

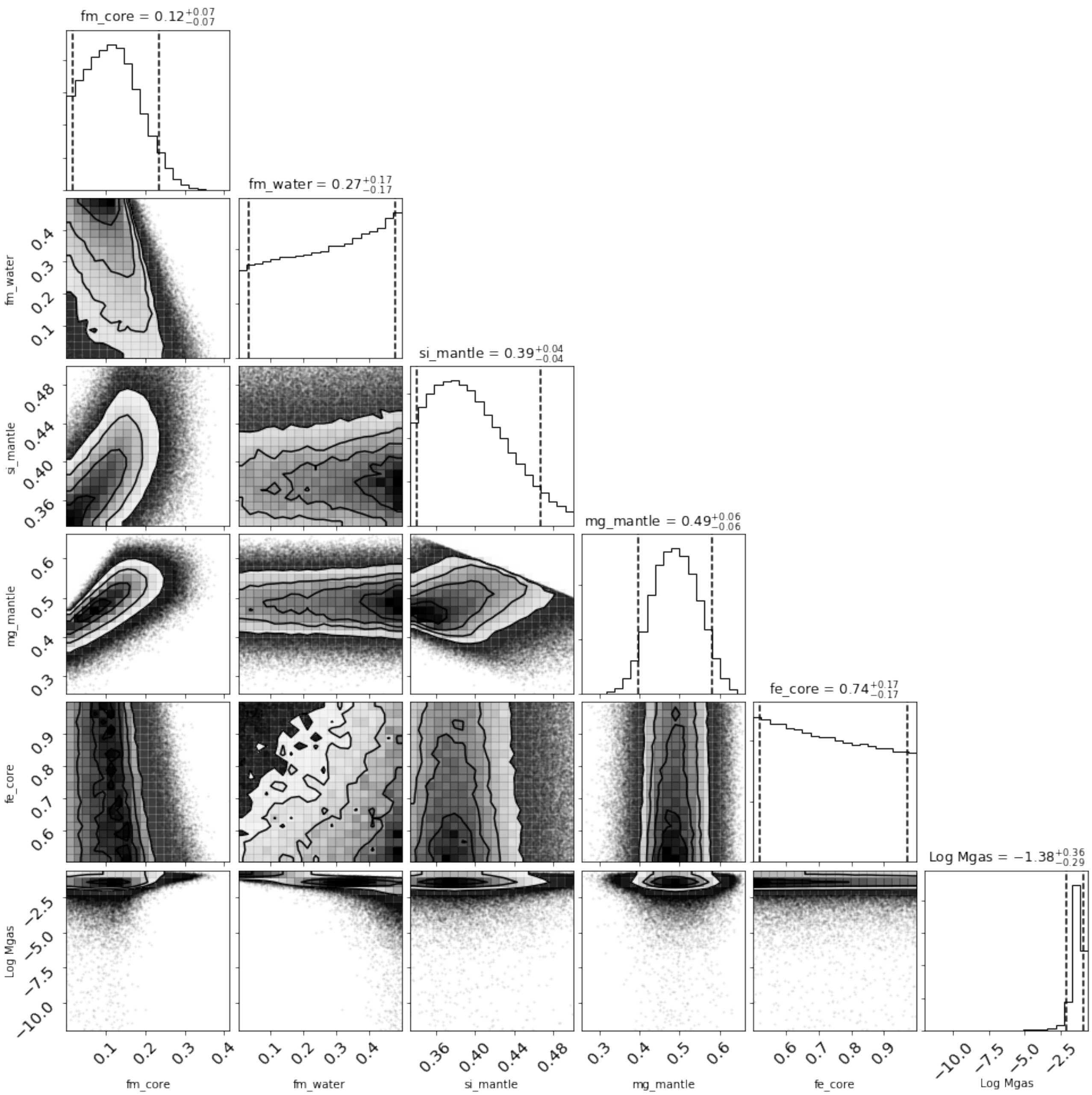

Supplementary Figure 14. Posterior distributions of the main internal structure parameters of planet d. The parameters are the same as in Supplementary Figure 12.

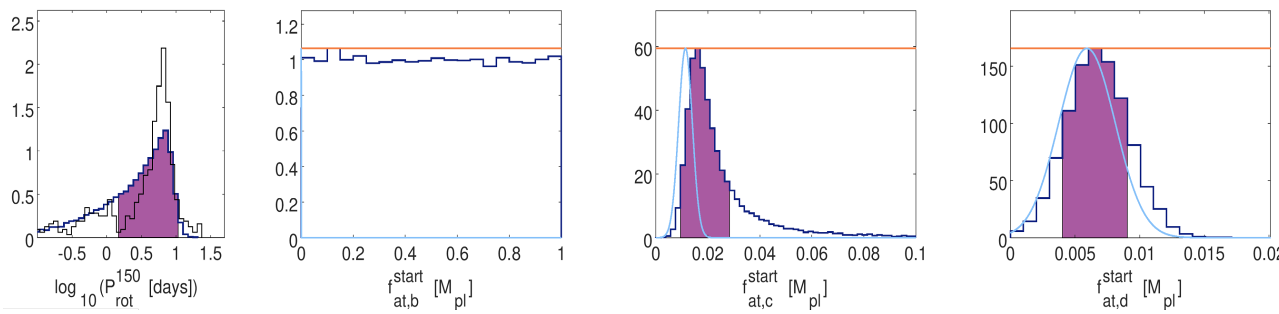

Supplementary Figure 15. *From left to right:* Posterior probability distribution functions (thick dark blue lines) for the stellar rotation period at an age of 150 Myr and for the initial atmospheric mass fractions of ν^2 Lupi b, c, and d. The purple areas indicate the 68% highest posterior density credible interval for each distribution. In the left panel, the distribution marked by the thin black line shows the stellar rotation period distribution[6] obtained from measurements of open cluster stars with an age of about 150 Myr and a mass within 0.1 $M_\odot$ of ν^2 Lupi's mass. In the right panels, the horizontal line represents the assumed flat prior arbitrarily shifted vertically to the highest point of each posterior for visualisation purposes. The bright blue line indicates the distribution of the current atmospheric mass fraction returned by our internal structure modelling. Based on this modelling, planet b has basically no gas. Therefore, the bright blue line is not visible in the plot for this planet.

References for the supplementary information

1. Kane, S. R. *et al.* Transits of Known Planets Orbiting a Naked-eye Star. *Astron. J.* **160**, 129 (2020). 2007.10995.

2. Foreman-Mackey, D. corner.py: Scatterplot matrices in python. *The Journal of Open Source Software* **1**, 24 (2016). URL https://doi.org/10.21105/joss.00024.

3. Chen, J. & Kipping, D. Probabilistic Forecasting of the Masses and Radii of Other Worlds. *Astrophys. J.* **834**, 17 (2017). 1603.08614.

4. Pereira, F. *et al.* Gaussian process modelling of granulation and oscillations in red giant stars. *Mon. Not. R. Astron. Soc.* **489**, 5764–5774 (2019). 1908.10662.

5. Sulis, S. *et al.* Mitigating flicker noise in high-precision photometry. I. Characterization of the noise structure, impact on the inferred transit parameters, and predictions for CHEOPS observations. *Astron. & Astrophys.* **636**, A70 (2020). 2003.07707.

6. Johnstone, C. P., Güdel, M., Brott, I. & Lüftinger, T. Stellar winds on the main-sequence. II. The evolution of rotation and winds. *Astron. & Astrophys.* **577**, A28 (2015). 1503.07494.